

Molecular and genetic diversity in the metastatic process of melanoma

Katja Harbst,^{1,2} Martin Lauss,^{1,2} Helena Cirenajwis,^{1,2} Christof Winter,^{1,2} Jillian Howlin,¹ Therese Törngren,¹ Anders Kvist,¹ Björn Nodin,³ Eleonor Olsson,¹ Jari Häkkinen,¹ Karin Jirstrom,³ Johan Staaf,^{1,2} Lotta Lundgren,^{1,4} Håkan Olsson,¹ Christian Ingvar,⁵ Sofia K Gruvberger-Saal,^{1,2} Lao H Saal^{1,2} and Göran Jönsson^{1,2,*}

¹ Department of Oncology, Clinical Sciences, Lund University, Sweden

² CREATE Health Strategic Centre for Clinical Cancer Research, Lund University, Sweden

³ Department of Pathology, Lund University and Skåne University Hospital, Lund, Sweden

⁴ Department of Oncology, Skåne University Hospital, Lund, Sweden

⁵ Department of Surgery, Lund University and Skåne University Hospital, Lund, Sweden

*Correspondence to: G Jönsson, Department of Oncology, Clinical Sciences, Lund University, Lund, Sweden. E-mail: goran_bjonsson@med.lu.se

Abstract

Diversity between metastatic melanoma tumours in individual patients is known; however, the molecular and genetic differences remain unclear. To examine the molecular and genetic differences between metastatic tumours, we performed gene-expression profiling of 63 melanoma tumours obtained from 28 patients (two or three tumours/patient), followed by analysis of their mutational landscape, using targeted deep sequencing of 1697 cancer genes and DNA copy number analysis. Gene-expression signatures revealed discordant phenotypes between tumour lesions within a patient in 50% of the cases. In 18 of 22 patients (where matched normal tissue was available), we found that the multiple lesions within a patient were genetically divergent, with one or more melanoma tumours harbouring 'private' somatic mutations. In one case, the distant subcutaneous metastasis of one patient occurring 3 months after an earlier regional lymph node metastasis had acquired 37 new coding sequence mutations, including mutations in *PTEN* and *CDH1*. However, *BRAF* and *NRAS* mutations, when present in the first metastasis, were always preserved in subsequent metastases. The patterns of nucleotide substitutions found in this study indicate an influence of UV radiation but possibly also DNA alkylating agents. Our results clearly demonstrate that metastatic melanoma is a molecularly highly heterogeneous disease that continues to progress throughout its clinical course. The private aberrations observed on a background of shared aberrations within a patient provide evidence of continued evolution of individual tumours following divergence from a common parental clone, and might have implications for personalized medicine strategies in melanoma treatment.

© 2014 The Authors. *The Journal of Pathology* published by John Wiley & Sons Ltd on behalf of Pathological Society of Great Britain and Ireland.

Keywords: melanoma; gene expression; deep sequencing; *BRAF*; *NRAS*

Received 19 August 2013; Revised 9 December 2013; Accepted 17 December 2013

No conflicts of interest were declared.

Introduction

Metastatic melanoma is an aggressive disease, notorious for its resistance to conventional therapy. Although development of targeted therapy in melanomas carrying *BRAF* mutations has revolutionized treatment, a significant number of patients with *BRAF* V600E metastatic melanoma experience recurrence within a few months upon treatment with the *BRAF* inhibitor vemurafenib [1] or the MEK inhibitor trametinib [2]. Treatment resistance could be explained by tumour heterogeneity, i.e. the existence of, or selection for, molecularly distinct subclones with metastatic capability. Supporting this hypothesis, intratumour heterogeneity has been reported in a vemurafenib-resistant subcutaneous melanoma metastasis, which contained a

subclone with a *de novo* *NRAS* mutation [3]. Colombino *et al* [4] have reported *BRAF* mutant metastases presumably seeded by a *BRAF* wild-type primary tumour and, more intriguingly, *BRAF* wild-type metastases in the presence of a *BRAF* mutant primary. Together, these findings indicate that some tumours may exhibit profound heterogeneity that contributes to the aggressive clinical course and eventual treatment resistance of melanoma. Indeed, large-scale sequencing studies of different solid cancers, including melanoma, have revealed extensive genetic heterogeneity between individual tumours [5–7]. In contrast to the prevailing theory of metastatic spread originating from the primary tumour at an advanced stage of the disease, recent evidence suggests the parallel development of the primary tumour and metastasis [8], or parallel development of multiple metastases in the same patient [9,10].

We recently identified four molecular subtypes of melanoma tumours using gene expression profiling characterized by differential expression of immune response genes, microphthalmia-associated transcription factor (*MITF*)-regulated genes and proliferation-related genes. These subtypes were named ‘pigmentation’ (*MITF*-high), ‘proliferative’ (*MITF*-low), ‘high-immune’ and ‘normal-like’; [11,12]. In the present study, we applied this subtype classification to multiple melanoma tumours from 28 patients previously diagnosed with a single primary melanoma (multiple metastases in 27 patients, and a primary tumour and metastasis in one patient). We identified 14 patients whose multiple tumours had divergent gene expression phenotypes. We further investigated the mutational landscape of the melanoma tumours from 22 of the 28 patients, using targeted gene sequencing and analysis of DNA copy number variation. Melanoma metastases from the same patient had a core of mutations and DNA copy number changes (herein termed ‘shared’ events). However, in all but four patients, mutations specific to one of the tumours within a patient were identified (‘private’ mutations). Our findings highlight the molecular and genetic diversity of metastatic melanoma tumours and indicate the need to redesign personalized medicine strategies for metastatic melanoma.

Material and methods

Patients

Tissue from melanoma tumours ($n=266$) and blood ($n=22$) were obtained from the Department of Oncology at Lund University. The samples were collected from melanoma patients referred to the Department of Surgery, Skåne University Hospital, for surgical removal of a melanoma tumour. From this cohort, 27 patients with multiple metastases (≥ 2) and one patient with a primary tumour and a subsequent metastasis were identified. With the exception of melanomas from one patient, all tumours were intermittently sun-induced melanomas or melanomas with an unknown primary ($n=5$). Clinical characteristics of the 28 patients are shown in Table 1. The study was approved by the ethics committee of the Lund University (Diary No. 101/2013).

Gene expression profiling

RNA from tumours ($n=266$) was subjected to microarray analysis. Tumours were classified into the four gene expression subtypes (pigmentation, proliferative, high-immune and normal-like), as previously described [11].

Next-generation sequencing

For targeted-capture deep sequencing (see supplementary material, Supplementary materials and methods, and Table S1, for sequencing data metrics), 1697

cancer genes were selected based on literature-documented association to cancer and the Catalogue of Somatic Mutations in Cancer (COSMIC) database (<http://www.sanger.ac.uk/genetics/CGP/cosmic/>; see supplementary material, Table S2). For details on targeted-capture deep sequencing, low-coverage whole-genome sequencing and DNA copy number analysis, see Supplementary materials and methods.

Results

Gene expression profiling reveals molecular diversity in multiple melanoma metastases following a single primary tumour

We attempted to characterize the molecular footprint of metastatic progression in malignant melanoma by a sequence of analyses on metastatic melanomas from patients with a single primary tumour (Figure 1A). Using microarray analysis, we analysed the gene-expression profiling of 266 melanoma tumours and identified 28 patients from whom at least two melanoma lesions diagnosed at different time points had been sampled (62 metastases in total; Table 1). We applied our previously described gene-expression signature [11,12] to the 62 melanoma lesions identified. In 14 of 28 patients (50%), melanoma metastatic tumours from the same patient belonged to different molecular subtypes (Table 1). Moreover, in four of these 14 patients, the later-occurring metastases had a proliferative phenotype, while the earlier tumours exhibited a pigmentation/high-immune/normal-like phenotype (patients 1, 17, 19 and 25). Notably, these proliferative-classified late melanoma metastases had a more advanced disease stage than the corresponding earlier tumour. For patient 25, both lesions were regional lymph node metastases; however, the first lesion was removed when the patient was diagnosed with regional metastatic disease, while the second lesion was removed when the patient was diagnosed with a generalized disease.

We never observed a change of molecular phenotype from the proliferative class in an earlier tumour to a different phenotypic class in a later metastasis, which indicates that the proliferative phenotype is associated with a late stage of the disease. For example, a local recurrence and a regional metastasis were collected for patient 19. The local recurrence was classified into the pigmentation phenotype, whereas the corresponding lymph node metastasis, diagnosed 4 years later, was classified into the proliferative phenotype. Patient 17 presented with a relatively thin primary melanoma (Breslow 1.65 mm) and 12 years later developed an in-transit metastasis that was classified as high-immune phenotype. A distant intestinal metastasis, diagnosed 2 years later, was classified into the proliferative phenotype.

Table 1. Molecular subtype and clinical characteristics of the 63 metastases

Age at dx	Primary tumour				Metastasis 1			Metastasis 2			Metastasis 3			
	Breslow (mm)	Clark	Type	Site	Date of dx	Type	Subtype	Date of dx	Type	Subtype	Date of dx	Type	Subtype	Date of dx
28	Patient 1 1.52	3	SSM ^s	Trunk	198907	Regional lymph node	Pigm	200103	Regional lymph node [#]	Prol	200106	Distant subcutaneous*	Prol	200109
46	Patient 2 4	4	NMM ^s	Trunk	199609	Regional lymph node	Pigm	199802	In transit lymph node [#]	Pigm	199807			
67	Patient 3 4	4	NMM ^s	Trunk	200603	In transit lymph node	Pigm	200608	Regional lymph node	High-imm	200611			
42	Patient 4 4	4	NMM ^s	Trunk	200711	Regional lymph node	Pigm	200802	Regional lymph node	Pigm	200904	Regional lymph node	Pigm	201011
63	Patient 5 2	N/A	N/A	Upper extremity	200006	Regional lymph node	Pigm	200804	Regional lymph node	Pigm	200903			
46	Patient 6 1.7	3	SSM	Trunk	200603	Regional lymph node	Pigm	200804	Distant lymph node	High-imm	200902			
60	Patient 7 1.7	3	NMM ^s	Lower extremity	200702	In transit lymph node	Pigm	200903	In transit lymph node	Pigm	201012			
NA	Patient 8 Unknown primary					In transit lymph node	Pigm	200810	In transit lymph node	Pigm	201005	In transit lymph node	Norm	201110
NA	Patient 9 Unknown primary					Lymph node	Pigm	200904	Distant	Norm	201012			
74	Patient 10 3.3	4	NMM ^e	Trunk	200903	Regional lymph node	High-imm	200907	Regional lymph node	High-imm	201003	Regional lymph node [#]	Norm	201105
NA	Patient 11 Unknown primary					Subcutaneous met	Pigm	200907	Lymph node	Pigm	200910			
NA	Patient 12 Unknown primary					Lymph node	Prol	201007	Lymph node	Prol	201011	Subcutaneous*	Prol	201110
42	Patient 13 3.4	3	NMM ^e	Trunk	200710	In transit subcutaneous	High-imm	201011	In transit subcutaneous	High-imm	201102			
77	Patient 14 3.5	3	SSM	Trunk	199601	Regional lymph node	High-imm	199609	Local recurrence	Pigm	199611	Local recurrence	High-imm	199702
80	Patient 15 12	3	NMM	Upper extremity	199409	Primary tumour	Prol	199409	Regional lymph node	Prol	199412			
61	Patient 16 2	3	N/A	Trunk	198908	Regional lymph node	Pigm	199411	Distant met	Pigm	199604			
64	Patient 17 1.65	3	SSM	Lower extremity	198507	Distant subcutaneous	High-imm	199705	Distant met	Prol	199904			
76	Patient 18 2.35	4	N/A	Lower extremity	199212	In transit subcutaneous	High-imm	199710	In transit subcutaneous	Pigm	199803			
31	Patient 19 1.4	4	SSM	Lower extremity	199405	Local recurrence	Pigm	199711	Regional lymph node	Prol	199806			
47	Patient 20 N/A	N/A	Acral	Nail	199711	Regional lymph node	Pigm	199712	Regional lymph node	Pigm	200407			
31	Patient 21 3.05	4	NMM	Upper extremity	199608	Distant subcutaneous	High-imm	199903	Distant subcutaneous	High-imm	200010			

Table 1. (Continued)

Age at dx	Primary tumour			Metastasis 1			Metastasis 2			Metastasis 3				
	Breslow (mm)	Clark	Type	Site	Date of dx	Type	Subtype	Date of dx	Type	Subtype	Date of dx	Type	Subtype	Date of dx
63	Patient 22 2.4	4	SSM	Trunk	199801	Regional lymph node	Prol	200008	Regional lymph node	Prol	200104	Regional lymph node	Prol	200104
61	Patient 23 7	4	NMM	Trunk	200011	Regional lymph node	High-imm	200108	Regional lymph node	Pigm	200109	Regional lymph node	Pigm	200109
NA	Patient 24 Unknown primary					Distant met	High-imm	200503	*Lymph node	Pigm	201111			
50	Patient 25 6	4	NMM [§]	Lower extremity	200001	Regional lymph node	High-imm	200504	Regional lymph node	Prol	200605	Regional lymph node	Prol	200605
73	Patient 26 11	4	NMM [€]	Lower extremity	200504	Regional lymph node	Prol	200505	Regional lymph node	Prol	200606	Regional lymph node	Prol	200606
75	Patient 27 3.4	4	SSM	Upper extremity	199605	Regional lymph node	Pigm	200511	Regional lymph node	High-imm	200612	Regional lymph node	High-imm	200612
192911	Patient 28 1.7	4	SSM	Lower extremity	200312	Regional lymph node	Prol	200606	Regional lymph node	Prol	200611	Regional lymph node	Prol	200611

[§]Primary ulcerated.

[€]Primary not ulcerated.

[#]Interferon treatment prior to detection of investigated lesion.

^{*}Chemotherapy treatment prior to detection of investigated lesion.
dx, diagnosis.

To confirm the observation of a tumour phenotype switch, we also performed unsupervised hierarchical clustering, using the 75% most variable genes across the entire dataset. Overall, 12 of 14 with no change in gene expression phenotype clustered as closest neighbours in the hierarchical dendrogram, and the results were significantly associated with the subtype (centroid) classification shown in Table 1 ($p = 0.049$, Fisher's exact test; see supplementary material, Figure S1).

Somatic mutations and copy number changes accompanying melanoma metastatic progression

Target enrichment and deep sequencing of all exons in 1697 genes (see supplementary material, Table S2) was performed on DNA samples from 49 tumours and matched blood from 22 patients included in the gene-expression analysis. Mean on-target sequence coverage of the tumour and normal DNA was 198x–594x (see supplementary material, Table S1), with 93–97% of targeted bases at 10x or higher coverage. Using VarScan somatic software [13], we detected 978 somatically acquired synonymous and non-synonymous single-nucleotide variants (SNVs), 21 indels in the coding sequence and 11 splice site mutations. We used CONTRA [14] to identify exon-specific copy number aberrations (CNAs; see supplementary material, Figure S2, Table S3).

First, we investigated the number of somatically acquired mutations in relation to progression of the disease in the 22 patients (Figures 1B, C, 2). Private mutations affected genes such as *CTNNB1*, *FBXW7*, *GRIN2A*, *TSC2*, *RUNX1* and *PTCH1* (for a list of identified mutations, see supplementary material, Tables S4–S25). *BRAF* and *NRAS* mutations, when present in the first metastasis, were always preserved in subsequent metastases. Patients with a tumour phenotype change to the proliferative class ($n = 3$) had a higher frequency of private mutations and CNAs (median 27, range 12–52) compared to patients without this phenotype change ($n = 19$) (median 9, range 0–29) ($p = 0.03$, Mann–Whitney test).

We investigated DNA CNAs in the tumours and found common losses on chromosome 9p and 10q corroborating previous studies on melanoma [15]. The single acral melanoma harboured *CDK4* amplification. Next, we searched for CNAs in genes known to be affected by CNAs in melanoma (*BRAF*, *KIT*, *MITF*, *CCND1*, *CDK4*, *PTEN*, *CDKN2A* and *AKT3*). None of the tumours showed focal amplifications of *AKT3*, *MDM2*, *KIT* or *MITF*. Two patients showed *CDK4* focal amplification and one patient had *CCND1* focal amplification; however, these were preserved in all three patients during progression. Frequent deletions and copy number gains were found in *CDKN2A*, *PTEN* and *BRAF*, with the majority of changes being preserved during progression. Differences were found in patient 1, where only the first metastasis had a heterozygous deletion of *CDKN2A*. A change in gene

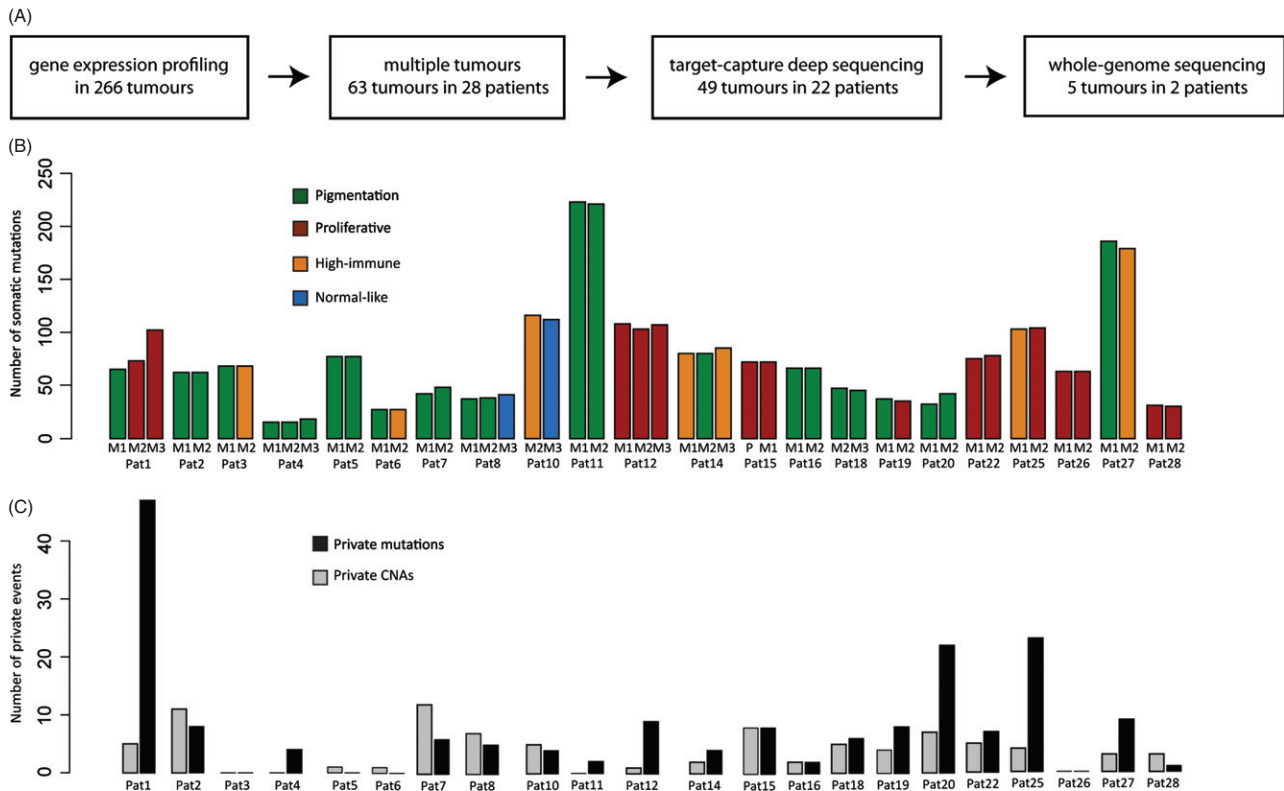


Figure 1. Study design depicting the molecular and genetic analysis of melanoma metastatic tumours. (A) Flow chart of the main methods used in the study. (B) Bar plot showing numbers of somatic mutations in multiple metastases from 22 patients. Each melanoma tumour was classified into the four gene expression phenotypes: pigmentation, green; proliferative, red; high-immune, orange; or normal-like, blue, and coloured accordingly. (C) Bar plot showing numbers of private copy number aberrations (CNAs) and mutations per patient. Private mutations within each patient were defined as being present in only one of the analysed tumours in the patient

expression phenotype was observed in this patient, where the first metastasis was classified in the pigmentation phenotype and the two latter metastases were classified in the proliferative class. Furthermore, in patient 27 the second metastasis had acquired additional *BRAF* gene copies. A change in gene expression phenotype occurred in this patient as well, where first metastasis was classified as pigmentation and second metastasis as high-immune response (see supplementary material, Figure S3).

Detailed analysis of somatic CNAs and chromosomal rearrangements in patients 1 and 2

Two patients (1 and 2) were selected for a more detailed investigation of the molecular footprint of metastatic progression. Patient 1 was selected on the basis of discordant subtype classification and a high number of private mutations (Figures 1B, 2). The three metastases displayed gradual loss of expression of pigmentation genes from M1 to M3, as shown by gene-expression analysis and MITF immunohistochemical (IHC) staining (Figure 3A, B). The gradual loss of MITF protein expression was reflected by a decrease in the number of MITF-positive melanoma cells in the tumour, with the least number of MITF-positive cells observed in M3. In patient 2, we found a low number of private mutations and both available metastases were

classified into the pigmentation subtype, corroborated by MITF IHC (Figure 4A, B).

To enrich our analysis for genomic rearrangements and CNAs, we performed low-coverage whole-genome sequencing of the five metastases in these two patients and matched lymphocyte DNA. Mean haploid genome sequence coverage was 1.9x–4.2x in these tumours (physical coverage 7.4x–13x). The metastases from each patient showed similar DNA copy number profiles (see supplementary material, Figure S4A), which indicates shared clonality of the tumours. We also observed a number of private aberrations. In patient 1, M2 and M3 shared many CNAs absent in M1, and vice versa, consistent with our previous results for these tumours [10]. The genomes of M2 and M3 diverged from that of M1 in 23 regions of differential copy number. Only one CNA, an 850 kbp gain at chromosome 3q13.31, was exclusive to M2, while none was specific to M3 (see supplementary material, Table S3, Figure S4A).

We also derived interchromosomal rearrangements, using BreakDancer [16]. To narrow down the candidate list, the positions of breakpoints were integrated with CNAs to isolate copy number change-supported interchromosomal rearrangements. This approach considerably decreased the number of candidate rearrangements suggested by BreakDancer, at the price of eliminating possible copy-number neutral rearrangements.

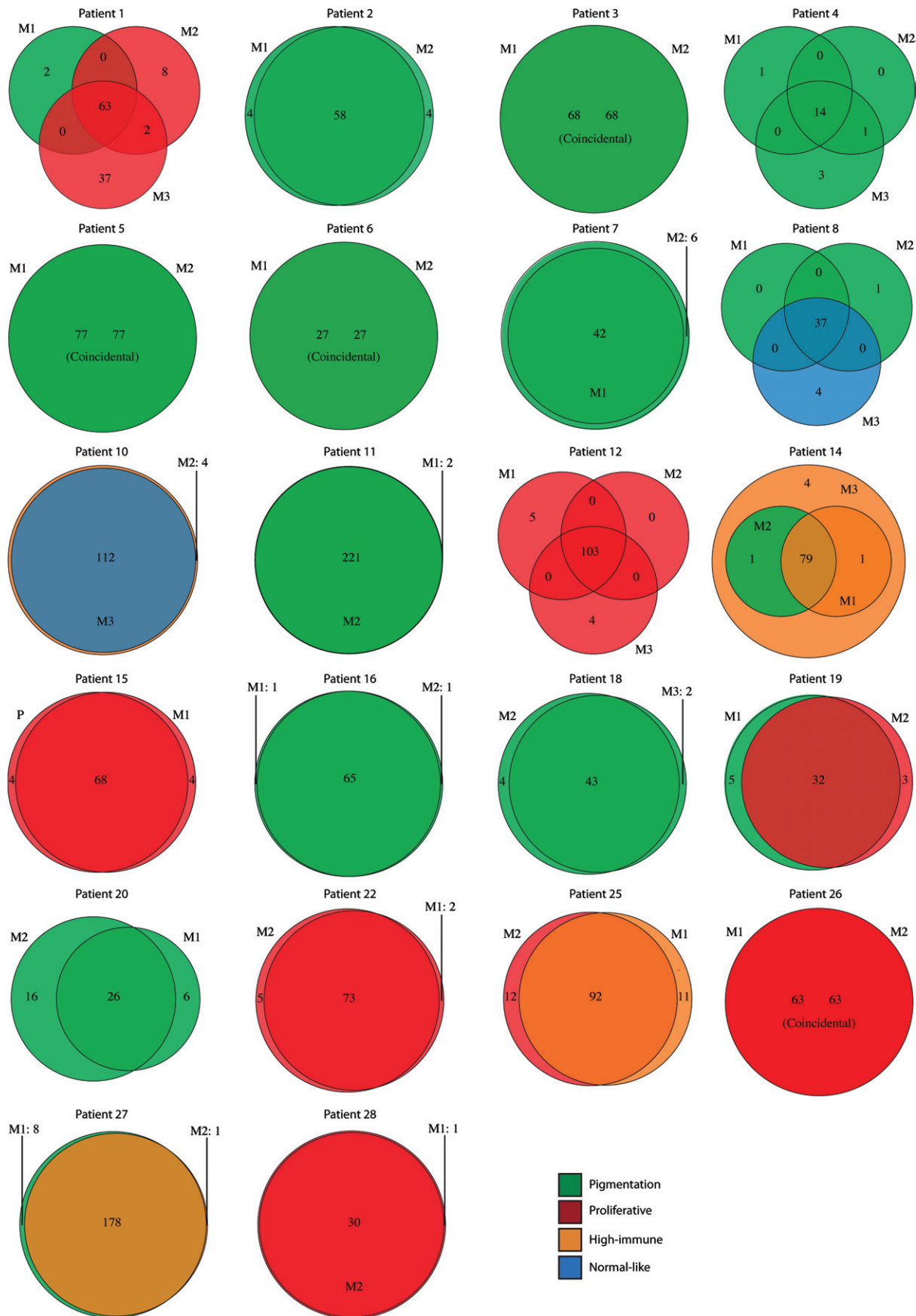


Figure 2. The mutational landscape of metastatic melanoma tumours: number of mutations (including shared and private somatic mutations) in the tumours of 22 patients depicted as Venn diagrams. The circle colours represent gene expression phenotypes: pigmentation, green; proliferative, red; high-immune, orange; or normal-like, blue. M1, metastatic lesion 1; M2, metastatic lesion 2; M3, metastatic lesion 3

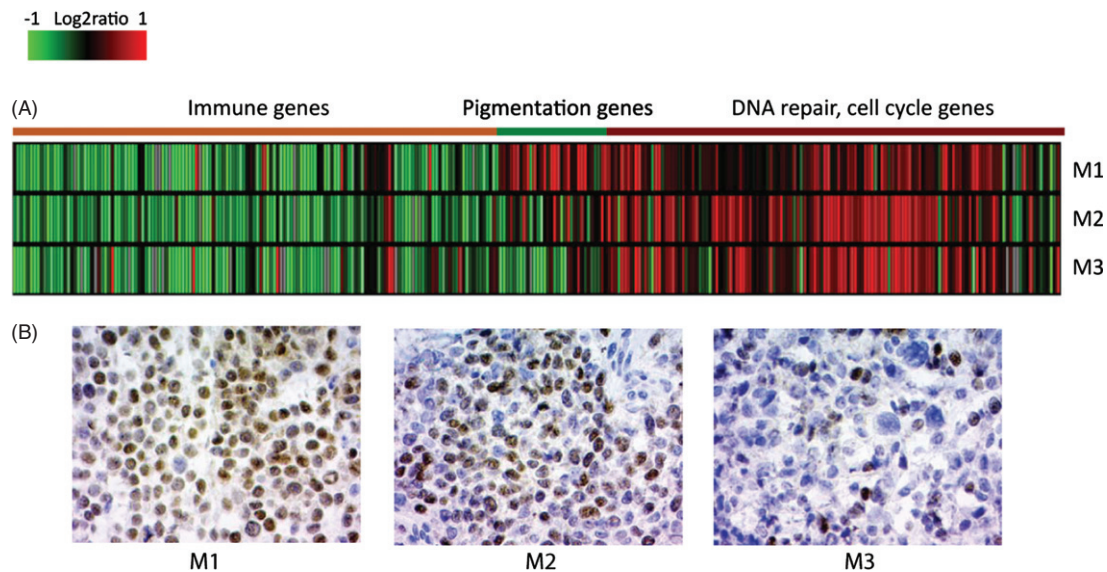


Figure 3. Molecular heterogeneity in patient 1. (A) Expression heat map of the subtype-specific genes in the melanoma metastases: red, over-expressed genes; green, down-regulated genes. (B) Microphthalmia-associated transcription factor (MITF) immunohistochemistry of metastatic tumour sections from patient 1. Cell nuclei are shown in blue. M1, metastatic lesion 1; M2, metastatic lesion 2; M3, metastatic lesion 3

We identified and validated by Sanger sequencing two interchromosomal rearrangements in patient 1 (see supplementary material, Figure S4). A genomic rearrangement involving chromosomes 7 and 15 was found in all three metastases, while a rearrangement between chromosomes 3 and 4 was exclusive to M1 (see supplementary material, Figure S4B). Moreover, the tumour genomes of all metastases from patient 1 were estimated as diploid by genome alteration print (GAP) analysis [17]. Together, these findings indicate common clonal origin of the metastases, while providing evidence for ongoing evolution of the cells forming the individual tumours. We identified and validated two interchromosomal rearrangements, both observed in M1 and M2 from patient 2: one between chromosomes 1 and 20, and another between chromosomes 2 and 20 (see supplementary material, Figure S4A). Although M1 and M2 from patient 2 were both estimated as triploid tumours by GAP analysis, they displayed only a few private mutations and did not change molecular phenotype; we identified many DNA CNA differences on chromosomes 2, 6, 7, 8, 12, 16, 17, 18, 20, 21 and 22, which indicated a continued evolution of the tumour genome (Figure 4C).

Somatic mutation patterns in metastatic progression in patients 1 and 2

The tumours from patient 1 shared 63 somatic exonic or splice site mutations (Figure 5A; see also supplementary material, Supplementary materials and methods). Among the shared alterations, notably, *RBI* harboured two mutations: a tandem GG > AA base substitution converting the tryptophan 516 into an immediate stop in exon 17, and a splice site mutation. Both mutations occurred in a gained chromosomal

region with copy number 3 in all three metastases. The variant allele frequencies in M1, M2 and M3 (nonsense, 30% in each; splice site, 55%, 55% and 65%, respectively) is consistent with inactivation of all three alleles, in a classic tumour suppressor inactivation manner.

In addition to this core of mutations, M1 carried two private exonic mutations, a synonymous substitution in *PRDM4* and *TRAPPC12*. M2 and M3 shared two mutations, including an oncogenic substitution in *PIK3CA*. In addition, M2 had eight private exonic mutations and M3 harboured 37 (Figure 5A; see also supplementary material, Supplementary materials and methods). Based on these findings, we present a progression model of patient 1, which is depicted in Figure 5B. The shared mutations appear at heterozygous allele frequency at diploid copy number (average 39–43%; see supplementary material, Figure S5) in the major clone of the tumours. However, the private mutations in M2 and M3 both appear in this group and at lower allele frequencies at diploid copy number, suggesting that additional subclone(s) evolved during progression (Figure 5B).

Of the 37 mutations private to M3, *PTEN* harboured a splice site mutation at 80% allele frequency that, together with chromosome 10 loss, likely contributed to the lower transcript level of *PTEN* observed in this tumour (see supplementary material, Table S26). While the presence of whole chromosome 10 hemizygous deletion in all three metastases implicates it as an early event in development of the precursor clone, the high allele frequency for the M3 private *PTEN* mutation points to it being a defining hit in the establishment of M3. Other notable mutations exclusively found in M3 were a frame-shift deletion in the DNA double-strand

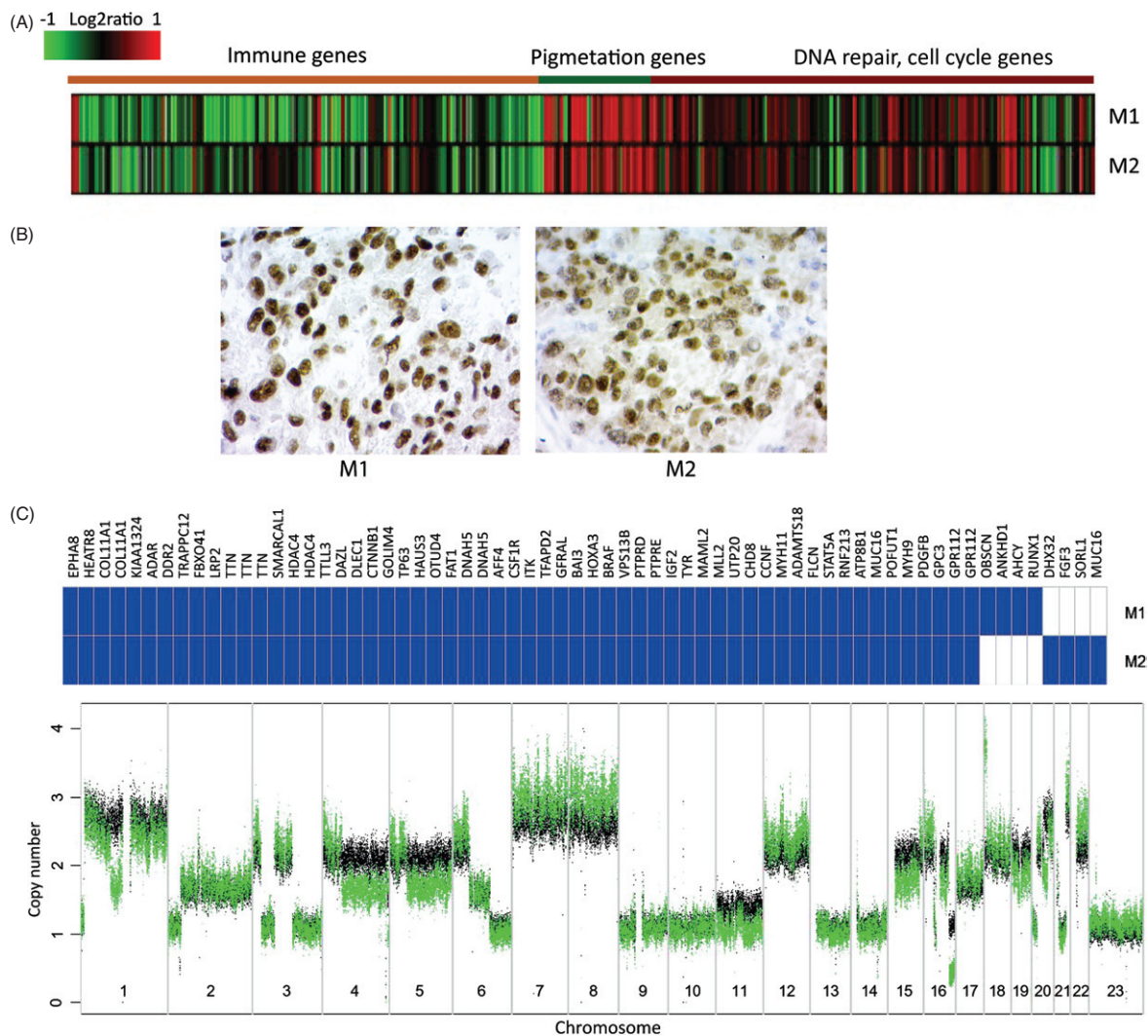


Figure 4. Molecular and genetic heterogeneity in patient 2. (A) Expression heat map of subtype-specific genes in the melanoma metastases. (B) Microphthalmia-associated transcription factor (MITF) immunohistochemistry in both metastases. (C) Mutated genes (blue) identified in metastases (upper panel). Genome-wide copy number profiles of M1 (black) and M2 (green) are superimposed onto each other and illustrate differences between the two metastases (lower panel)

break (DSB) repair gene *RAD50* and a *CDH1* splice site mutation.

For patient 2, both metastases belonged to the pigmentation phenotype. They shared 58 mutations, including *BRAF* V600E, and contained few private mutations (M1, 4; M2, 4) (Figure 4C; see also supplementary material, Supplementary materials and methods). For example, a missense mutation in *RUNX1*, which encodes a transcription factor frequently mutated in leukaemia, was found only in M1.

The within-patient shared mutations in all 22 patients were predominantly of the C:G \rightarrow T:A type (range 64–94%, median 89%). This transition has been repeatedly reported to be the predominant type of base substitution in diverse types of cancer [18]. The sites of the shared C:G \rightarrow T:A mutations were usually preceded by another pyrimidine at the 5' position (Figure 5C), pointing towards UV-induced DNA damage as the mechanism of mutation [19], in line with previous studies in melanoma [6,7]. In patient

1, 94% (63/67) of the shared exon or splicing SNVs were of this type. Notably, the base substitution pattern of SNVs private to M3 deviated from this pattern: A:T \rightarrow G:C transitions constituted 80% (24/30) of the M3 private SNVs (significant enrichment, as compared to shared mutations; Fisher's test, $p < 0.0001$; and to M1/M2 private mutations, $p = 0.014$). We investigated the close-range sequence context of these sites, by comparing base composition within a 10-position window around the mutation site to that of 500 randomly picked coding A/T sites. The base composition of the +1 and +2 positions was significantly different from that of the random sites (Fisher's test, Benjamini–Hochberg adjusted $p = 0.007$ and $p = 0.009$, respectively). This non-random pattern suggests an as-yet unknown mutation mechanism that needs further investigation. The private mutations found in the other patients did not display the A:T \rightarrow G:C pattern, but instead displayed the classical UV-induced pattern C:G \rightarrow T:A.

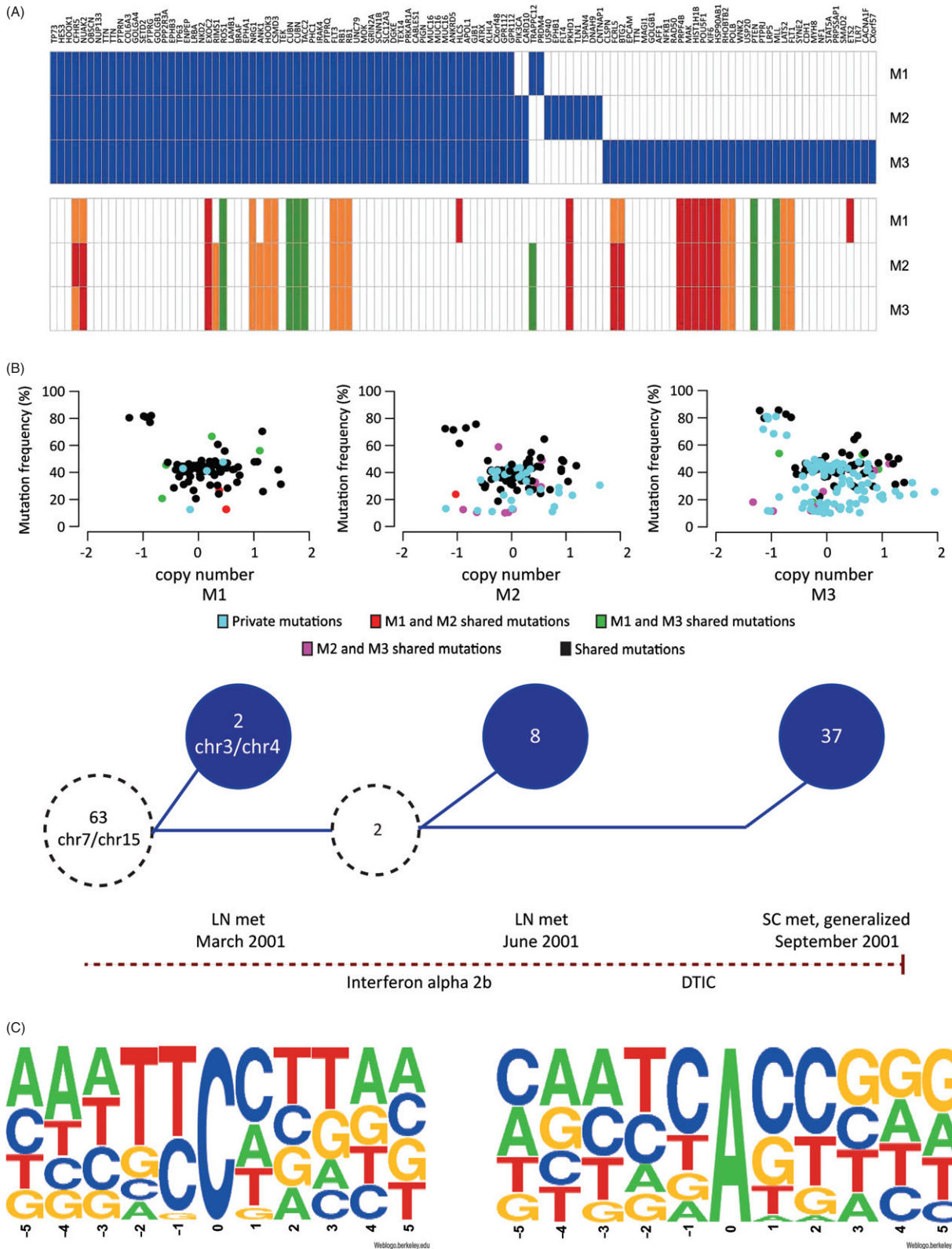


Figure 5. Genetic heterogeneity in patient 1. (A) Mutated genes (upper panel, blue) and corresponding copy number (lower panel) in the three metastases from patient 1. Copy number: white = 2, green = 1, orange = 3, red = 4 inferred from GAP results. (B) Progression model: (upper panel) Somatic mutations (exonic, splice-site and intronic) plotted by log₂ copy number (x axis) versus variant allele frequency (y axis); colours are indicated in the legend; (lower panel) the common precursor clone (dotted circle on the far left) contained 63 exonic or splice site mutations and a rearrangement involving chromosomes 7 and 15, all found in all three metastases. M1 harboured two private mutations and another genomic rearrangement, between chromosomes 3 and 4. Hypothetical common predecessor of M2 and M3 (smaller dotted circle) developed from the precursor clone and contained two additional mutations. Finally, M2 acquired eight additional private exonic mutations, and M3 37 additional private mutations. Red dotted line represents time, with diagnoses and treatments indicated; LN, lymph node; SC, subcutaneous; met, metastasis; DTIC, dacarbazine. (C) Sequence context of shared (all three metastases, left) and M3 private (right) mutations demonstrates clear pattern differences

Discussion

Using molecular and genetic analysis of multiple metastatic melanoma lesions from 28 patients, we provide evidence of a heterogeneous gene-expression pattern between different metastatic lesions and, in 82% of patients, occurrence of private mutations. We found that known driver mutations, such as oncogenic *BRAF* and *NRAS* mutations, were always somatically preserved, whereas others (such as *PTEN* and *CTNNB1*) were somatically acquired during progression. Our findings highlight molecular and genetic diversity in the metastatic process that might hinder personalized genomic strategies in melanoma, based on single tumour biopsies.

From a comprehensive set of 266 melanoma tumours subjected to gene-expression profiling, we identified 28 patients with at least two melanoma lesions diagnosed at different time points. Classification of tumours into our previously described phenotypes, based on gene-expression profiles [11,12], showed that 50% of these patients had metastases belonging to different phenotypes. We observed that tumours of the proliferative phenotype were of a more advanced stage than the corresponding earlier tumour, indicating that the described molecular phenotypes might reflect a progression model of melanoma. However, this notion needs to be verified in larger cohorts. We did not identify any patients with metastases belonging to different phenotypes that had the first metastatic tumour classified into the proliferative phenotype. Interestingly, we found decreased expression of melanocyte differentiation markers in proliferative classified tumours, which indicate that a dedifferentiation process might be involved in the switch from MITF-high phenotype to a MITF-low (proliferative) phenotype (Figure 3B). Combined analysis of gene-expression data with results from targeted deep sequencing from patient 1 suggest a continued tumour evolution, exemplified by accumulation of additional mutations and by molecular phenotype switching in later metastases. Our findings further support the idea of phenotype switching previously described in experimental melanoma model systems [20,21]. However, based on our findings, we cannot conclude that molecular phenotype switching is associated with an increased amount of somatically acquired mutations during tumour progression.

Further supporting our data, protein expression studies have shown extensive heterogeneity in a primary melanoma [22] and intra-tumour heterogeneity has also been shown in renal cell carcinoma using whole-exome sequencing [8]. On the extreme end of tumour evolution is the late-occurring metastasis three (M3) in patient 1, with 37 private coding sequence mutations. This high mutation rate was not reflected at the level of general genomic instability, as the copy number profile of M3 is almost identical to that of M2 from patient 1. This lack of correlation between the numbers of mutations and CNAs within a tumour has been reported

previously [23]. However, we only investigated a part of the genome (5.5 Mb) for mutations and, although improbable, it is possible that some of the tumours preferentially acquired mutations in other genes. Furthermore, the mutation frequency of the newly acquired mutations in M2 and M3 from patient 1 was found at a wide range (10–80%), indicating the evolution of both major and minor clones. Indeed, we found a *PTEN* mutation at allele frequency of 80%, indicating its presence in the major clone in M3 of patient 1.

The presence of the strong UVR mutagenesis signature in all tumours was consistent with previous studies in melanoma [6,7,23]. By contrast, the majority (24/30) of the patient 1, M3 private base substitutions were of the A:T → G:C type. Although the aetiology of this substitution to our knowledge remains unknown, the over-representation and the non-random distribution of the bases at the +1 and +2 positions speaks against a stochastic process and in favour of the action of an internal or external agent. Whether this effect is mediated by the alkylating agent dacarbazine (DTIC), which was used to treat the patient between the M2 and M3 diagnoses, remains to be investigated. Of note, DTIC has been described to mainly induce C:G → T:A transitions [24,25]. This mutational signature might also be attributed to ADAR-like DNA deaminases [26] or MLH1-deficiency [27]. Further studies are required to determine the significance and context of this mutational signature.

In summary, we have provided evidence for a complex metastatic process of melanoma. The genetic and molecular diversity observed in metastatic melanoma tumours challenge personalized genomic strategies that are based on single tumour biopsies. In melanoma, research on resistance to novel therapeutic options (such as *BRAF* inhibition) has resulted in identification of several molecular alterations that confer resistance. Whether these mechanisms are acquired or somatically preserved remains to be determined. However, our results highlight the molecular and genetic heterogeneity of melanoma tumours and the capacity of melanoma cells to adapt to external agents. Identification of shared molecular patterns may contribute to more robust biomarkers, as well as treatment-predictive markers.

Acknowledgements

This study was supported by the Swedish Cancer Society, the Swedish Research Council, BioCARE, the Berta Kamprad Foundation, the Gunnar Nilsson Cancer Foundation, the Gustav Vth Jubilee Foundation and Governmental Support for Medical Research (ALF). The authors thank the editors at Elevate Scientific for helpful comments on the article.

Author contributions

KH, ML, HC and GJ designed the study; KH, HC, TT, BN, KJ and GJ carried out experiments; KH, ML, CW,

JH, AK, EO, JH, JS and GJ analysed data; LL, HO and CI collected material; and KH, ML, HC, CW, JH, AK, JS, SGS, LS and GJ interpreted data. All authors were involved in writing the paper and had final approval of the submitted version.

Abbreviations

CN, copy number; CNA, copy number aberration; DSB, double-strand break; DTIC, dacarbazine; IHC, immunohistochemical; FDR, false-discovery rate; SNV, single-nucleotide variant; UVR, ultraviolet radiation; UVB, ultraviolet B radiation.

References

- Sosman JA, Kim KB, Schuchter L, *et al.* Survival in *BRAF* V600-mutant advanced melanoma treated with vemurafenib. *N Engl J Med* 2012; **366**: 707–714.
- Flaherty KT, Robert C, Hersey P, *et al.* Improved survival with MEK inhibition in *BRAF*-mutated melanoma. *N Engl J Med* 2012; **367**: 107–114.
- Wilmott JS, Tembe V, Howle JR, *et al.* Intratumoral molecular heterogeneity in a *BRAF*-mutant, *BRAF* inhibitor-resistant melanoma: a case illustrating the challenges for personalized medicine. *Mol Cancer Ther* 2012; **11**: 2704–2708.
- Colombino M, Capone M, Lissia A, *et al.* *BRAF/ NRAS* mutation frequencies among primary tumors and metastases in patients with melanoma. *J Clin Oncol* 2012; **30**: 2522–2529.
- Nik-Zainal S, Alexandrov LB, Wedge DC, *et al.* Mutational processes molding the genomes of 21 breast cancers. *Cell* 2012; **149**: 979–993.
- Hodis E, Watson IR, Kryukov GV, *et al.* A landscape of driver mutations in melanoma. *Cell* 2012; **150**: 251–263.
- Krauthammer M, Kong Y, Ha BH, *et al.* Exome sequencing identifies recurrent somatic *RAC1* mutations in melanoma. *Nat Genet* 2012; **44**: 1006–1014.
- Gerlinger M, Rowan AJ, Horswell S, *et al.* Intratumor heterogeneity and branched evolution revealed by multiregion sequencing. *N Engl J Med* 2012; **366**: 883–892.
- Katona TM, Jones TD, Wang M, *et al.* Genetically heterogeneous and clonally unrelated metastases may arise in patients with cutaneous melanoma. *Am J Surg Pathol* 2007; **31**: 1029–1037.
- Harbst K, Staaf J, Masback A, *et al.* Multiple metastases from cutaneous malignant melanoma patients may display heterogeneous genomic and epigenomic patterns. *Melanoma Res* 2010; **20**: 381–391.
- Harbst K, Staaf J, Lauss M, *et al.* Molecular profiling reveals low- and high-grade forms of primary melanoma. *Clin Cancer Res* 2012; **18**: 4026–4036.
- Jonsson G, Busch C, Knappskog S, *et al.* Gene expression profiling-based identification of molecular subtypes in stage IV melanomas with different clinical outcome. *Clin Cancer Res* 2010; **16**: 3356–3367.
- Koboldt DC, Zhang Q, Larson DE, *et al.* VarScan 2: somatic mutation and copy number alteration discovery in cancer by exome sequencing. *Genome Res* 2012; **22**: 568–576.
- Li J, Lupat R, Amarasinghe KC, *et al.* CONTRA: copy number analysis for targeted resequencing. *Bioinformatics* 2012; **28**: 1307–1313.
- Curtin JA, Fridlyand J, Kageshita T, *et al.* Distinct sets of genetic alterations in melanoma. *N Engl J Med* 2005; **353**: 2135–2147.
- Chen K, Wallis JW, McLellan MD, *et al.* BreakDancer: an algorithm for high-resolution mapping of genomic structural variation. *Nat Methods* 2009; **6**: 677–681.
- Popova T, Manie E, Stoppa-Lyonnet D, *et al.* Genome Alteration Print (GAP): a tool to visualize and mine complex cancer genomic profiles obtained by SNP arrays. *Genome Biol* 2009; **10**: R128.
- Greenman C, Stephens P, Smith R, *et al.* Patterns of somatic mutation in human cancer genomes. *Nature* 2007; **446**: 153–158.
- Pfeifer GP, You YH, Besaratinia A. Mutations induced by ultraviolet light. *Mutat Res* 2005; **571**: 19–31.
- Hoek KS, Schlegel NC, Brafford P, *et al.* Metastatic potential of melanomas defined by specific gene expression profiles with no *BRAF* signature. *Pigment Cell Res* 2006; **19**: 290–302.
- Widmer DS, Cheng PF, Eichhoff OM, *et al.* Systematic classification of melanoma cells by phenotype-specific gene expression mapping. *Pigment Cell Melanoma Res* 2012; **25**: 343–353.
- Eichhoff OM, Zipsper MC, Xu M, *et al.* The immunohistochemistry of invasive and proliferative phenotype switching in melanoma: a case report. *Melanoma Res* 2010; **20**: 349–355.
- Berger MF, Hodis E, Heffernan TP, *et al.* Melanoma genome sequencing reveals frequent *PREX2* mutations. *Nature* 2012; **485**: 502–506.
- Marchesi F, Turriziani M, Tortorelli G, *et al.* Triazene compounds: mechanism of action and related DNA repair systems. *Pharmacol Res* 2007; **56**: 275–287.
- Alexandrov LB, Nik-Zainal S, Wedge DC, *et al.* Signatures of mutational processes in human cancer. *Nature* 2013; **500**: 415–421.
- Muramatsu M, Kinoshita K, Fagarasan S, *et al.* Class switch recombination and hypermutation require activation-induced cytidine deaminase (AID), a potential RNA editing enzyme. *Cell* 2000; **102**: 553–563.
- Lee H, Popodi E, Tang H, *et al.* Rate and molecular spectrum of spontaneous mutations in the bacterium *Escherichia coli* as determined by whole-genome sequencing. *Proc Natl Acad Sci USA* 2012; **109**: E2774–2783.

SUPPLEMENTARY MATERIAL ON THE INTERNET

The following supplementary material may be found in the online version of this article:

Supplementary materials and methods

Figure S1. Hierarchical clustering of melanoma samples. (A) Unsupervised clustering using the 75% most variable genes. (B) Clustering using the centroid genes

Figure S2. Copy number profiles of the melanoma metastatic tumours, based on CONTRA analysis of the targeted deep-sequencing data

Figure S3. DNA copy number changes in melanoma-relevant genes across the patients

Figure S4. Various types of somatic alterations identified in the tumours of patients 1 and 2, using whole-genome sequencing

Figure S5. Variant allele frequencies of the shared and M3 private mutations in patient 1

Table S1. Sequencing data metrics

Table S2. Genes ($n = 1697$) in the target enrichment panel

Table S3. Regions of differential copy number between metastases in patient 1

Tables S4–25. Coding sequence (exonic and splice site) mutations in patients 1–28

Table S26. Processed microarray expression data on multiple metastases

Table S27. Raw microarray expression data

25 Years ago in the *Journal of Pathology*

Protamine sulphate-induced proteinuria: The roles of glomerular injury and depletion of polyanion

Aurora Messina, Davtd J. Davies and Professor Graeme B. Ryan

Antigenic specificity of human alveolar macrophages and blood monocytes studied by an immunofluorescence technique

Britt Nakstad, Torstein Lyberg, Kåre Baklien and Nils P. Boye

Histological evidence of natural killer cell aggregation against malignant melanoma induced by adoptive immunotherapy with lymphokine-activated killer cells

T. Yamamura, Y. Fujitani, T. Kawauchi, E. Wada, Y. Kobayashi, K. Yoshikawa, H. Ogawa, H. Sugiyama, M. Ohsawa and Dr K. Aozasa

The relationship between the distribution of lymphoid cells in the skin and in vitro adhesion to connective tissue

Dr A. S. Jack and K. Jane Chapman

To view these articles, and more, please visit:

www.thejournalofpathology.com

Click 'ALL ISSUES (1892 - 2011)', to read articles going right back to Volume 1, Issue 1.

The Journal of Pathology
Understanding Disease

